Journal of Alloys and Compounds 504 (2010) 134–140

Contents lists available at ScienceDirect

Journal of Alloys and Compounds

journal homepage: www.elsevier.com/locate/jallcom

Direct synthesis of Mg–Ni compounds from their oxides

Serdar Tan, Kadri Aydınol, Tayfur Öztürk*, İshak Karakaya

Department of Metallurgical and Materials Engineering, Middle East Technical University, Ankara 06531, Turkey

ARTICLE INFO

Article history:
Received 13 December 2009
Received in revised form 9 May 2010
Accepted 15 May 2010
Available online 27 May 2010

Keywords:
Electroreduction
Magnesium oxide
Nickel oxide
Electrical conductivity
Mg_2Ni
$MgNi_2$

ABSTRACT

A study was carried out on the synthesis of Mg–Ni compounds as well as on the extraction of pure Ni and Mg from their oxides using the method of electro-deoxidation. The oxides sintered at 1200 °C were in the form of discrete phases NiO and MgO, suitably proportioned to yield Ni, $MgNi_2$, Mg_2Ni and Mg. The oxides were electrolyzed at 3.2 V in a eutectic mixture of $CaCl_2$–NaCl solution maintained at a constant temperature (900–600 °C), using a graphite anode. The study has shown that NiO rich mixture, MgO:NiO = 1:2, can be reduced successfully to metallic state. Some loss of Mg was apparent in the latter, with the result that the product was far from the target composition $MgNi_2$. The electroreduction of MgO rich mixtures was difficult to achieve. The mixture MgO:NiO = 2:1 when electrolyzed at 725 °C for 24 h, could be reduced to metallic phases only in small proportions (18 wt.%). In pure MgO, no trace of reduction was observed during the electrolysis at 600 °C. Difficulties in the electroreduction of MgO and MgO rich mixtures were partially attributed to low conductivity of MgO.

1. Introduction

Solid state electroreduction of oxides has been an area of intense research during the last decade [1–4]. The method was used not only to extract metals from their oxides [1] but also to synthesize alloys and compounds from the oxide mixtures [2]. In this method, pellets of oxide powders used as the cathode were deoxidized by the application of a potential against graphite without decomposing the electrolyte, a molten salt that is capable of dissolving and transporting oxygen ions. During electrolysis, while oxygen ions are removed from the pellets and transported to the anode to form either CO and/or CO_2, metallic constituents are left behind in the cathode, which via in situ reactions may yield alloys or compounds. The method has the advantage that when inert anodes are used, the electrolysis leads to oxygen generation rather than CO or CO_2 emission [5].

A number of factors affect the ease with which the reduction is achieved in the electro-deoxidation process. It has been reported that, oxides of low reduction potentials, e.g. NiO, Cr_2O_3, Fe_2O_3, are deoxidized faster than others, e.g. rare earth oxides [6]. The ease of reduction is also affected by the oxygen diffusivity in the solid state. Oxides such as TiO_2 and ZrO_2 are reduced relatively easily in the early stages, but as pointed out by Chen et al. [7], once the metallic state is achieved, the rate slows down, since the diffusion of oxygen is extremely slow in the metallic lattices. Insulating oxides such as SiO_2 was also difficult to reduce and required the number of contacting points in the cathode to be increased [8]. Here the reduction is claimed to proceed via the propagation of conductor–insulator–electrolyte triple interline [9,10]. Similarly, the deoxidation of some oxides, such as MgO and Al_2O_3, has been found to be complicated due to difficulties in the initial metallization of the oxide pellets as well as due to the fact that the corresponding metals have low melting points [11].

The reduction of oxide mixtures is often more complicated than their pure counterparts. The mixtures, such as Tb_2O_3–NiO [12], Fe_2O_3–TiO_2 [13] and TiO_2–NiO [14], have been successfully deoxidized to yield the respective intermetallic compounds, i.e. $TbNi_5$, FeTi, and TiNi. The complication often arises because the oxides are reduced at different rates which may give rise to separate individual phases rather than to the compounds themselves. Yong et al. [14] reported that the use of a higher reduction potential may reduce the differences in the reduction rates and could thus promote the compound formation. In this context, the pre-compounding of the oxide mixtures as well as the optimization of the porosity in the pellets could be beneficial to have more complete reduction of the oxides to the required stoichiometry. The reduction of the oxide mixtures also has its advantages. For instance, compounds, such as Ni_2MnGa [15] and Nb_3Sn [16], have been successfully synthesized in the solid state at temperatures higher than the melting points of some of their constituent metals. Furthermore, Qui et al. [17] points out that the reducibility of the oxide mixture could be improved by fast reduction of one of the oxide phases and the formation of metallic particles in situ may enhance the reduction of the other oxide constituents.

---

* Corresponding author. Tel.: +90 312 210 5935; fax: +90 312 210 2518.
E-mail address: ozturk@metu.edu.tr (T. Öztürk).

0925-8388/$ – see front matter © 2010 Elsevier B.V. All rights reserved.
doi:10.1016/j.jallcom.2010.05.071

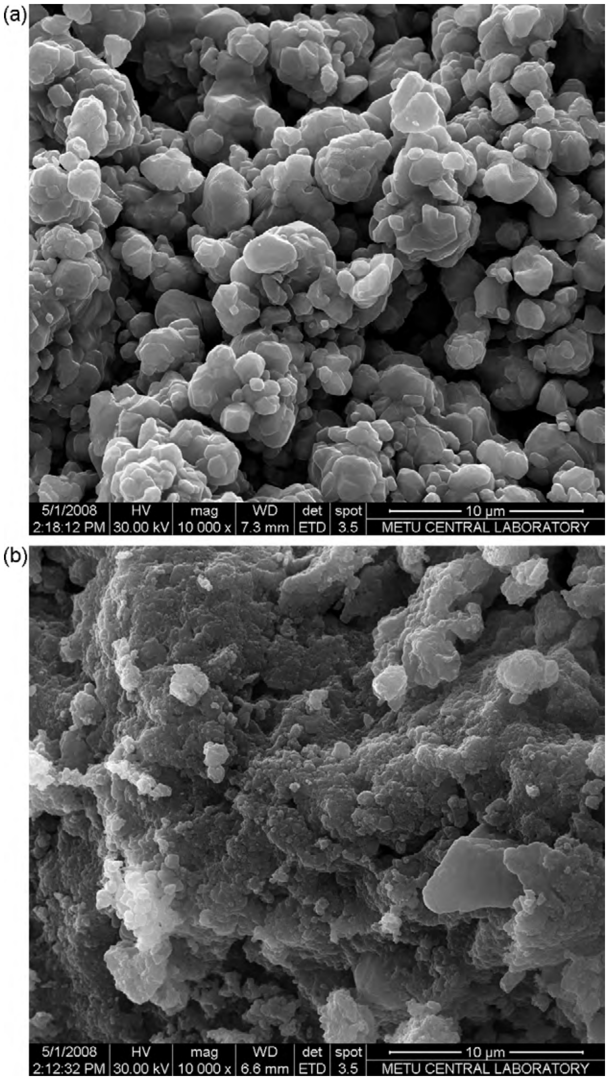

Fig. 1. SEM images of oxide powders; (a) NiO and (b) MgO used in the experiments.

The current work deals with synthesis of Mg–Ni compounds as well as the extraction of pure Ni and Mg from their oxides. The study is of particular interest since the system involves oxides, MgO and NiO, which have widely different physical, such as electrical conductivity and oxygen diffusivity, and thermodynamic properties. Therefore, electro-deoxidation of these oxides, either on their own or as mixtures, are of considerable significance. Moreover, Mg_2Ni, one of the target compounds has a considerable potential as hydrogen storage alloy [18].

2. Experimental

Starting materials were NiO (99%, Alfa Aeser) and MgO (99%, Merck) powders. NiO powders were irregular in shape and 1.20 μm in size, Fig. 1(a). MgO particles were much finer, i.e. sub-micron in size, Fig. 1(b). Both powders, in the as-supplied form, were agglomerated to larger granules with average sizes, measured by a laser diffraction technique, of D_{50} of 18 μm and 30 μm for NiO and MgO, respectively.

Oxide powders were mixed in fixed proportions corresponding to metallic compositions: Ni, $MgNi_2$, Mg_2Ni and Mg. The mixing was carried out for 30 min in a Spex Mill at ball-to-powder ratio (B/P) of 1. The mixtures were further hand mixed with some PVA solution and allowed to air dry for 24 h. They were then cold-compacted under a pressure of 110 MPa to cylindrical pellets of 15 mm in diameter and 4–7 mm in height. All pellets were heated to 1200 °C with a heating rate of 5 °C/min and sintered for 6 h.

Deoxidation experiments were conducted in a stainless steel reactor placed in a vertical furnace. The reactor comprises a stainless steel crucible for holding molten electrolyte and has a lid with retractable electrodes immersible into the electrolyte. Two sets of electrodes were available, one set (auxiliary) for pre-electrolysis and the other (working electrodes) for electro-deoxidation, Fig. 2. Anode-to-cathode distance in both pairs was 25 mm. Anodes were graphite rods, 13 mm of diameter and 40 mm in length, and were connected to a stainless steel current collector. The cathodes were stainless steel wire of 4 mm in diameter, which in the case of working electrode was connected to the oxide pellet. The reactor was sealed, allowing electrolysis in an argon atmosphere (99.995% purity) maintained at a flow rate of 150–250 ml/min.

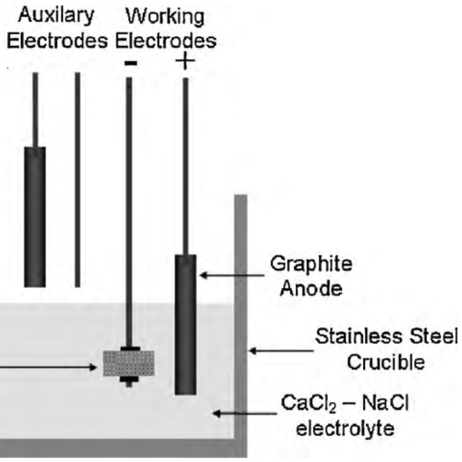

Fig. 2. Schematic drawing of an electrolytic cell used in the deoxidation experiments.

A eutectic mixture of $CaCl_2$–NaCl was used as the electrolyte, which has a melting point of about 505 °C. Approximately 1 kg of electrolyte was used for each experiment. The salt mixture was heated slowly to the electrolysis temperature to reduce its moisture content. The electrolyte was further purified by pre-electrolysis using the auxiliary electrodes at a potential of 3.0 V for a minimum of 6 h. Following the pre-electrolysis, the auxiliary electrodes were lifted above the electrolyte, and the electrolysis was initiated by immersing the working electrodes, i.e. oxide pellet (cathode) and a fresh graphite rod (anode) into the salt bath. During electrolysis, current-time data was collected by a computer connected to the power supply.

At the end of each experiment, the electrodes were disconnected from the electrical supply and both the graphite anode and the reduced sample were removed from the electrolyte by positioning them above the melt. After cooling to room temperature under a continuous flow of argon gas, the reactor lid was opened and the sample with its stainless steel connector was removed. The sample was washed in a hot methanol–ethanol–water mixture and all undissolved material was collected for XRD and SEM analysis.

Volumetric porosities of the oxide pellets after sintering were determined from geometric dimensions and the mass of the pellets, making use of specific density values of the constituent oxides. Phase make-up of the samples was determined via X-ray diffraction. The quantity of phases was determined following Rietveld refinements of the powder diffraction patterns using the software MAUD [19].

3. Results and discussion

The oxides following the sintering treatment yielded pellets with porosity values varying between 37 and 57%. An X-ray diffractogram of a sintered pellet of mixed oxide MgO:NiO = 1:2 is given in Fig. 3(a). Since MgO and NiO have the same crystal structure and very similar lattice parameters, the peaks are very close to one another showing considerable overlapping. Still, the peaks of MgO and NiO are differentiated from each other, indicating that the mixed oxides have a two-phase structure rather than a single-phase solid solution. Considering that the sintering was carried out at 1200 °C this is somewhat surprising and could be due to insufficient mixing of the oxides in the SPEX mill. This has been further verified via SEM imaging in backscattered mode. Regions of two different contrasts were apparent, see Fig. 3(b), in compliance with the presence of two-phase structure. Grains in the sintered samples had sizes (mean intercept value) of 1.9 μm and 3.2 μm for MgO and NiO respectively.

The process of electroreduction leads to the discharging of oxygen from the cathode thus leaving the metallic constituents behind. More specifically, under the applied potential, the oxygen is ionized

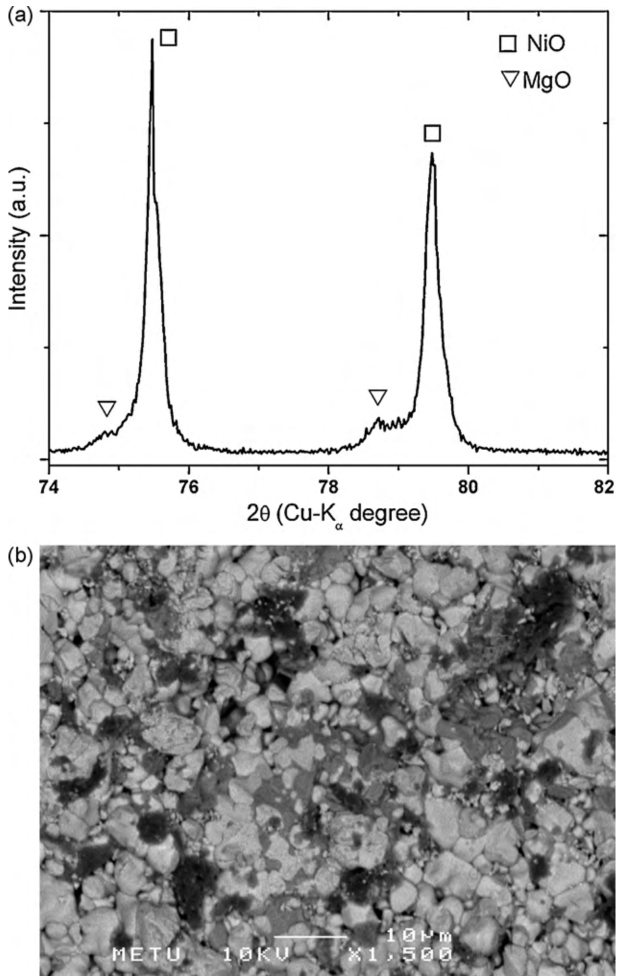

Fig. 3. MgO:NiO = 1:2 pellet sintered at 1200 °C for 6 h; (a) X-ray diffractogram, (b) SEM image recorded in back scattered electron mode indicating a two-phase structure; NiO (bright phase) and MgO (gray phase). Black regions are pores.

(either directly from the cathode [1] or through calcium deposited onto the cathode [3,4]), dissolved in the electrolyte and is discharged at the anode (carbon) where it forms CO or CO_2. Standard reduction potentials, ΔE°, of oxides (MgO and NiO) for both CO and CO_2 evolution and the standard decomposition potentials of electrolyte ($CaCl_2$ and NaCl) were calculated from the thermodynamic data given in [20,21] and are shown in Table 1. The potentials calculated for oxides for the case of intermetallic formation, i.e. $MgNi_2$ and Mg_2Ni, are also included in the table. Here ΔE° values of the overall reactions, in volts, were directly calculated from:

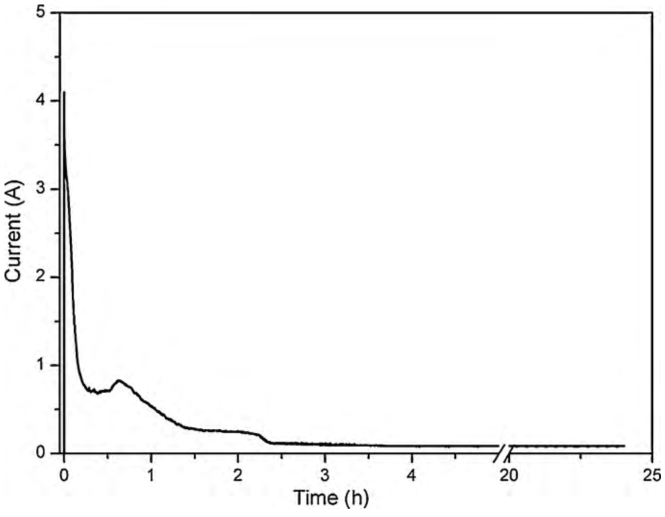

Fig. 4. Current–time data collected during electro-deoxidation of NiO at 900 °C with 3.2 V.

$$\Delta E^\circ = -\frac{\Delta G^\circ}{nF}$$

Here ΔG° is the standard Gibbs free energy change of the reaction (in Joules) at temperature T, n is the number of electrons transferred in the balanced electrochemical reaction, and F is the Faraday's constant (96,500 Coulombs/gram equivalent), assuming that the components are in pure state.

The data, given in Table 1, indicates that the reduction potential of NiO is positive and therefore it is expected to reduce more easily. The electro-deoxidation of MgO on the other hand requires the application of a relatively high potential. It should also be noted that at 900 °C, the reactions leading to CO evolution are more favorable whereas at lower temperatures, e.g. 600 °C, the more favorable reactions are those leading to CO_2 evolution. The data in Table 1 further shows that the choice of 3.2 V used in the current experiments is safely below the decomposition potentials of both $CaCl_2$ and NaCl at 600 °C and 725 °C. This voltage is quite close to the decomposition potentials of the electrolyte at 900 °C. The decomposition voltage of NaCl given in Table 1 at 900 °C is in fact slightly less than 3.2 V but this value refers to the pure state. The value calculated for NaCl decomposition in equimolar solution of $CaCl_2$–NaCl by using an activity coefficient of NaCl as 0.66 [22] is 3.27 V, which is above the current applied potential. Furthermore, the addition of IR drop,

Table 1
Standard reduction potentials of MgO, NiO and CaO and decomposition potentials of $CaCl_2$ and NaCl calculated at temperatures of 900 °C, 725 °C and 600 °C. The data in parenthesis refers the potential when the metal is in liquid state. For details, see text. Standard reduction potentials of reactions yielding the intermetallics $MgNi_2$ and Mg_2Ni are also shown. The reactions are given in the order of increasing reduction potentials at 725 °C.

Reaction	ΔE° (V)		
	600 °C	725 °C	900 °C
$NiO_{(s)} + C_{(s)} = Ni_{(s)} + CO_{(g)}$	+0.16	+0.26	+0.43
$NiO_{(s)} + 0.5C_{(s)} = Ni_{(s)} + 0.5CO_2$	+0.20	+0.25	+0.33
$MgO_{(s)} + 2NiO_{(s)} + 3C_{(s)} = MgNi_{2(s)} + 3CO_{(g)}$	−0.36	−0.24	−0.09
$2MgO_{(s)} + 4NiO_{(s)} + 3C_{(s)} = 2MgNi_{2(s)} + 3CO_{2(g)}$	−0.32	−0.26	−0.18
$2MgO_{(s)} + NiO_{(s)} + 3C_{(s)} = Mg_2Ni_{(s,l)} + 3CO_{(s)}$	−0.98	−0.86	(−0.70)
$4MgO_{(s)} + 2NiO_{(s)} + 3C_{(s)} = 2Mg_2Ni_{(s,l)} + 3CO_{2(g)}$	−0.94	−0.87	(−0.78)
$MgO_{(s)} + C_{(s)} = Mg_{(s,l)} + CO_{(g)}$	−1.64	(−1.52)	(−1.34)
$MgO_{(s)} + 0.5C_{(s)} = Mg_{(s,l)} + 0.5CO_{2(g)}$	−1.60	(−1.53)	(−1.43)
$CaO_{(s)} + C_{(s)} = Ca_{(s,l)} + CO_{(g)}$	−1.83	−1.71	(−1.52)
$CaO_{(s)} + 0.5C_{(s)} = Ca_{(s,l)} + 0.5CO_{2(g)}$	−1.79	−1.72	(−1.63)
$NaCl_{(l)} = Na_{(l)} + 0.5Cl_{2(g)}$	(−3.37)	(−3.28)	(−3.16)
$CaCl_{2(l)} = Ca_{(s,l)} + Cl_2$	−3.40	−3.32	(−3.21)

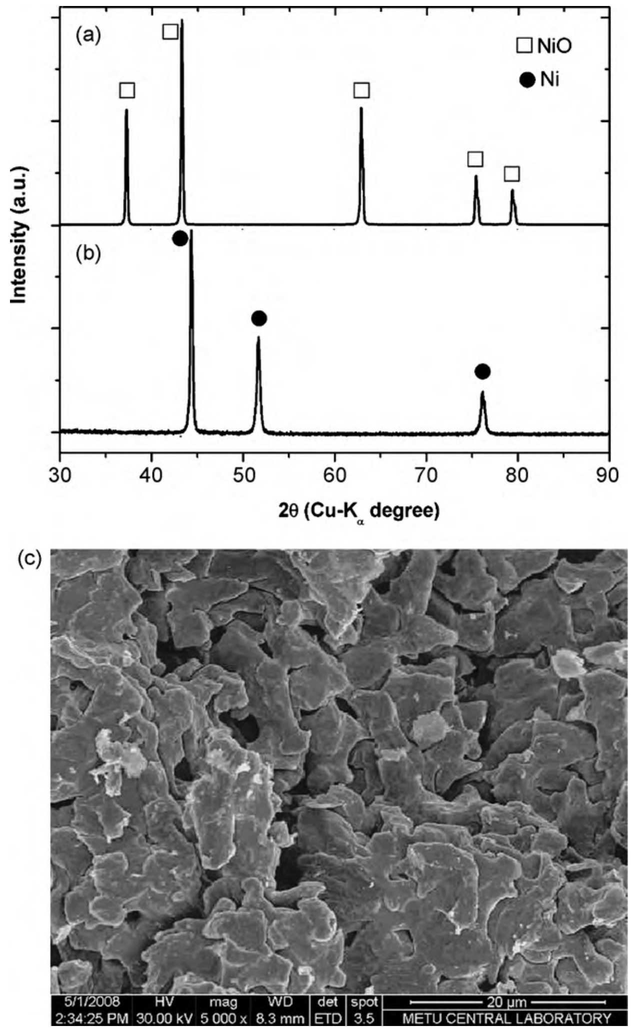

Fig. 5. NiO pellet; X-ray diffractogram of the sample (a) before and (b) after electro-deoxidation, at 900 °C for 24 h (3.2 V). (c) Refers to SEM image of the reduced sample.

anodic and cathodic overpotentials to the above value makes the actual decomposition voltage even greater than 3.27 V.

Current–time curve recorded during deoxidation of NiO pellet at 900 °C is given in Fig. 4. As seen from the plot, the current shows an initial transient rise, and over a period of 30 min it settles down to a steady state, which then cascades down to smaller values. After 3 h, the current reduces to a residual value of 0.1 A that continues to drop at a very slow rate until the end of the electrolysis (24 h).

X-ray diffractograms of the NiO pellet before and after electro-deoxidation for 24 h at 900 °C are given in Fig. 5(a) and (b). As seen in the diffractograms, the pellet was reduced successfully to pure Ni. The SEM image of the pellet, given in Fig. 5(c), shows metallic powders in a sintered state, with particle sizes ranging from 5 μm to 10 μm. Deoxidation of NiO for 24 h at 725 °C and 600 °C was successful in yielding pure Ni.

The oxide mixture with a target composition of $MgNi_2$, i.e. MgO:NiO = 1:2, was deoxidized at 900 °C. X-ray diffractogram of the resulting product, given in Fig. 6(a), contained metallic constituents and residual MgO, indicating that the reduction was not yet complete. The metallic constituents were $MgNi_2$, i.e. the target composition, and a pure Ni. Detailed analysis of XRD pattern showed that the fractions of phases were; 50 wt.%, 44 wt.% and 6 wt.% for $MgNi_2$, Ni and MgO, respectively. The presence of residual MgO (but not NiO) reveals that the reduction of NiO proceeded faster than that of MgO. SEM image of the product given in Fig. 6(b) shows again a particulate structure, less coarse than that obtained from electro-deoxidation of pure NiO.

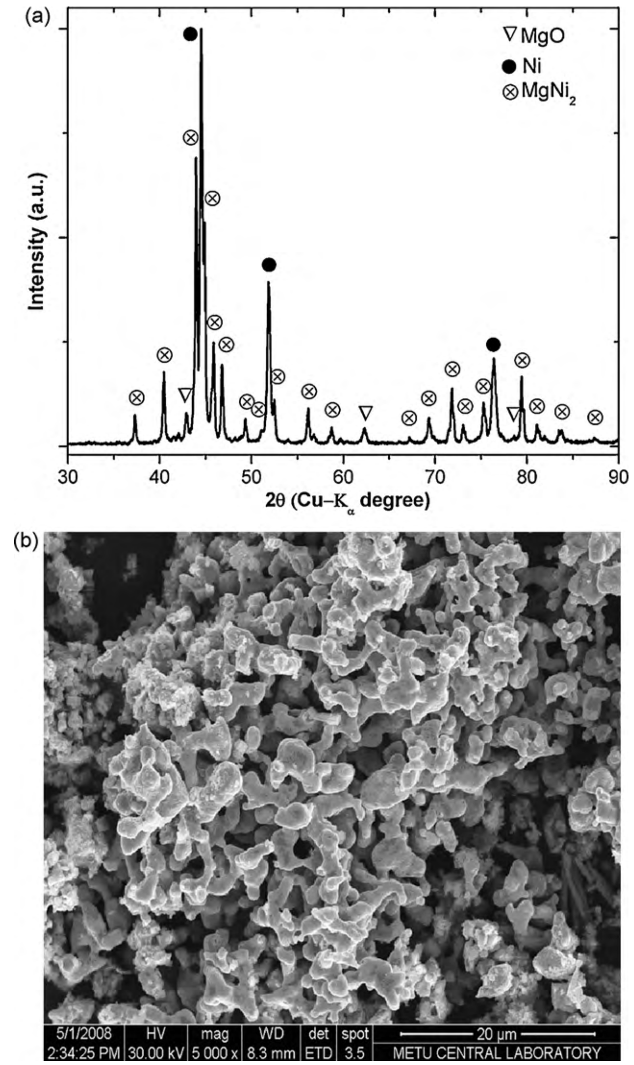

Fig. 6. MgO:NiO = 1:2 pellet; (a) X-ray diffractogram and (b) SEM image of powders after electro-deoxidation for 24 h at 900 °C with 3.2 V.

Although the oxide mixture MgO:NiO = 1:2 after the electrolysis contains a certain fraction of MgO, this fraction is not enough to convert all Ni into $MgNi_2$. This implies that a certain fraction of MgO either in partially or fully reduced form was lost from the cathode, probably as a result of dissolution in the electrolyte. This was checked by examining a sample taken from the electrolyte after the electrolysis. The sample was dissolved in water and the resulting residue was analyzed by EDS. The amount of Mg when scaled for 1 kg of electrolyte was approximately 0.09 g. This is nearly 15% of the total Mg in the cathode.

The mixture MgO:NiO = 2:1 could not be electrolyzed at 900 °C, since the target composition Mg_2Ni is liquid at that temperature. The experiments were therefore carried out at 725 °C, safely below the melting point of Mg_2Ni (760 °C). As given in Fig. 7(a), the pellet, after 24 h of electrolysis, contained only a small fraction of metallic phases: Mg_2Ni, $MgNi_2$ and Ni. The rest, i.e. 82 wt.% of the sample, was unreduced oxides. The final pellet was easy to grind and SEM image of the pulverized product, given in Fig. 7(b), had a non-metallic appearance. In the case of pure MgO, electro-deoxidation was even more difficult. The electrolysis carried out at 600 °C did not lead to any reduction. No trace of Mg could be detected in the sample after 24 h of electrolysis at 3.2 V.

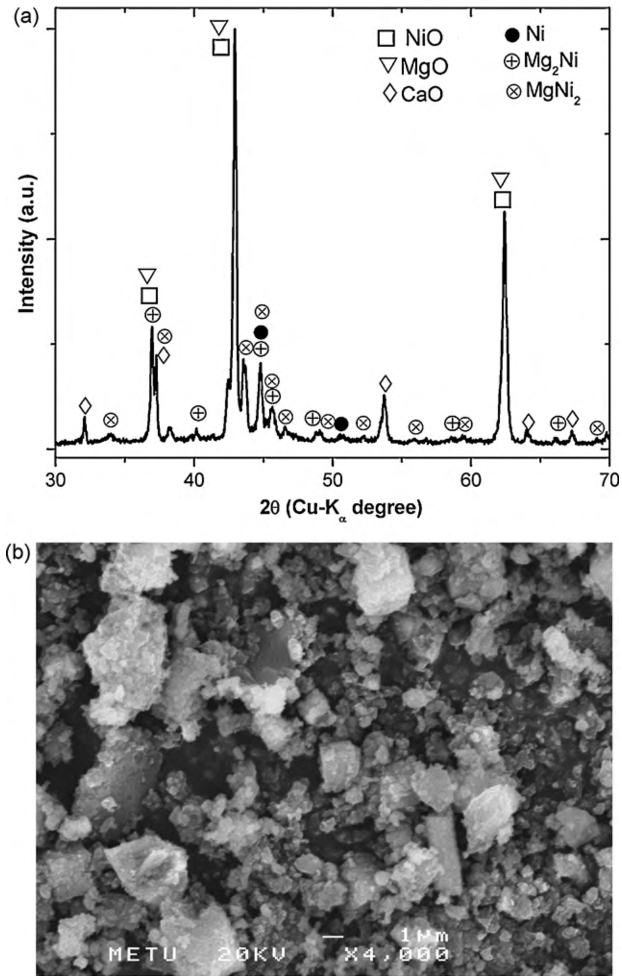

Fig. 7. MgO:NiO = 2:1 pellet; (a) X-ray diffractogram and (b) SEM image of powders obtained after electro-deoxidation for 24 h at 725 °C with 3.2 V.

In an attempt to reduce the MgO rich mixtures, separate experiments were carried out; in which the potential was raised to 5 V. This value is well above the decomposition potential of the electrolyte. Fig. 8 shows the current–time plot recorded for MgO:NiO = 2:1 mixture. As seen in the figure, the current fluctuates quite erratically, probably as a result of more than one reduction reactions, e.g. reactions leading to gas evolution at anode [23]. The experiment was quite successful for MgO:NiO = 2:1 mixture. The pellet electrolyzed for 24 h at 600 °C was reduced almost fully to the metallic state. The phases were Mg_2Ni, $MgNi_2$, $Mg(OH)_2$ and a small amount of residual MgO (5 wt.%). The presence of $Mg(OH)_2$ is probably due to the reaction of metallic Mg with H_2O used to separate reduced pellet from the salt after electrolysis. The experiment with pure MgO, however, was not as successful. The electrolysis with 5 V at 600 °C yielded only a trace amount of Mg_2Ca and $Mg(OH)_2$, both adding up to about 1 wt.%, the rest being MgO. Thus, even the application of 5 V was not enough to reduce the MgO pellet.

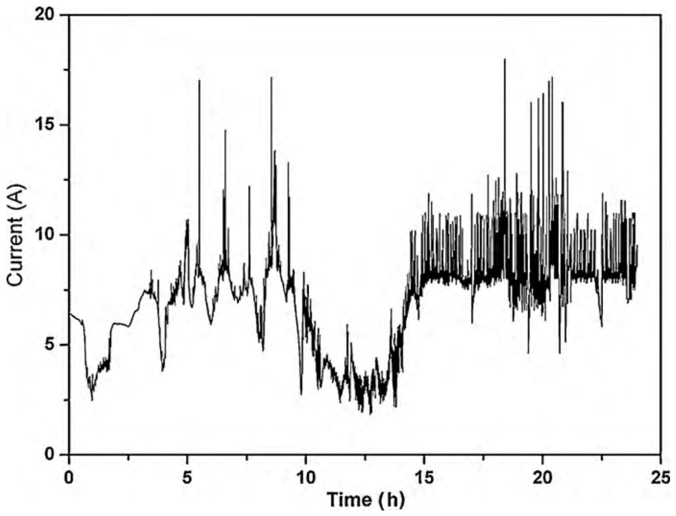

Fig. 8. Current–time data collected during electro-deoxidation of MgO:NiO = 2:1 effected with 5 V at 600 °C.

Returning to the results obtained with 3.2 V, it should be pointed out that, of the four metallic phases aimed in the current work, the ease of reduction closely parallels the values of the standard reduction potentials reported in Table 1. The reactions in the table were listed according to their reduction potentials (at 725 °C). Accordingly, the reductions become more and more difficult as one moves from Ni-rich compositions to Mg rich ones.

The ease of reduction in NiO could be attributed to its low, in fact positive, reduction voltage as well as to the other factors such as its high conductivity (see below). Similar observations were made in a study by Qiu et al. [24] in which 100–200 μg of NiO powders were reduced successfully within a few minutes at 900 °C.

The oxide mixture targeted for $MgNi_2$ was also reduced relatively easily. Here, the difficulty was in the production of samples with desired stoichiometry since there was some loss of Mg from the cathode during the electrolysis. Still, the electrolysis of MgO:NiO = 1:2 mixture is not unlike that of NiO, i.e. the mixture resulted in a reduction which is nearly complete. Also, as NiO has very low reduction potential, formation of a Ni-rich environment in the pellet probably enhanced the reduction of MgO in the oxide mixture. Similar arguments were put forward by Ma et al. [25] and Yong et al. [14] in explaining the enhanced reduction of TiO_2 in the presence of Fe_2O_3 and NiO.

The loss of Mg during the electrolysis appears to be the major obstacle for the desired quantity of compound formation. Conditions in the pellet should be such that Mg upon reduction should react with Ni, which had been reduced earlier in the process, forming the targeted compound. Circumstances that favor compound formation are well documented in the earlier studies. One approach is to carry out the electrolysis under high potential. In such conditions as explained by Yong et al. [14], the differences in the reduction rate of the oxides are diminished and all elements are extracted in the same time scale, which would allow them to react with one another resulting in the compound formation. The other approach is the solutionizing of the oxide mixture itself [17,24]. In this case, the metallic species being present in the same oxide phase are close to each other, which upon reduction could react easily with one another. The latter approach would be particularly suitable for the current system since the oxides NiO–MgO have complete solid solubility. Thus, it is possible to form MgO and NiO in a single-phase structure in which Mg:Ni ratio can be adjusted to any preselected value.

Current experiments show that the reduction of MgO via electro-deoxidation is an extremely difficult task. This is true for the mixture targeted for Mg_2Ni as well as that for the pure Mg. MgO:NiO = 2:1 mixture for instance after 24 h of electrolysis yielded only a small fraction of metallic phases, four-fifths of the pellet still remained as oxides. This implies that the phases in the oxide mixture do not behave independently. If they were, NiO could have been reduced to pure Ni totally, leaving behind MgO. In a pellet with porosity in the order of 40% or so, this situation could be partially attributed to the insufficient conductivity of the pellet.

To check this, the electrical conductivities of the oxide pellets were measured with a two-probe technique. The results, given

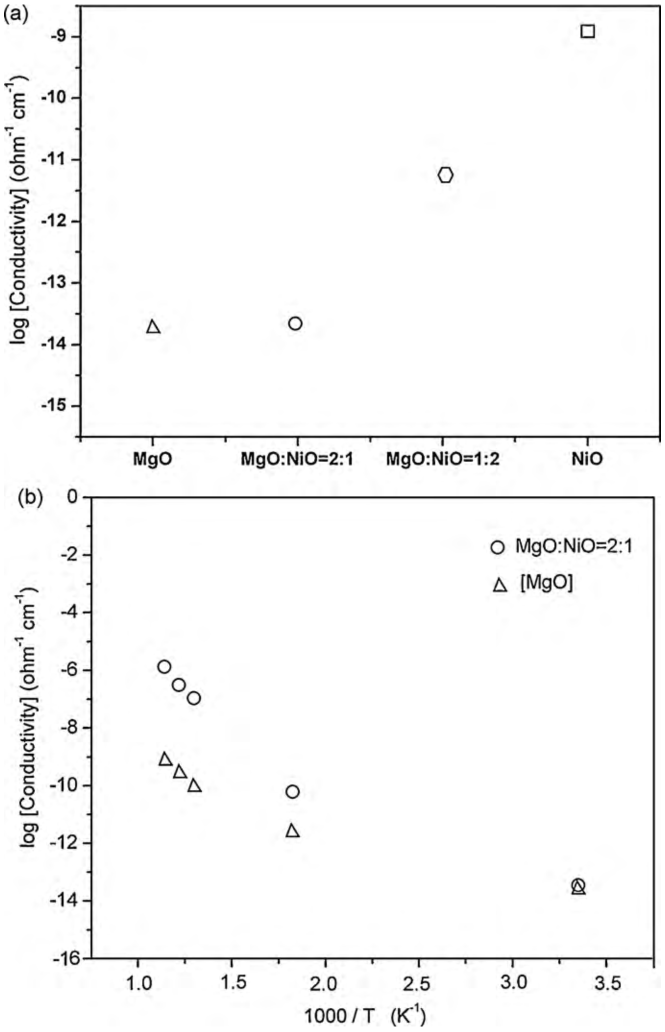

Fig. 9. (a) Electrical conductivities of MgO, MgO:NiO = 2:1, MgO:NiO = 1:2 and NiO at room temperature, and (b) conductivity values as a function of temperature up to 600 °C for MgO and MgO:NiO = 2:1.

in Fig. 9(a), verify that the conductivity of MgO differs drastically from that of NiO. The value for MgO at room temperature is close to 10^{-14} ohm^{-1} cm^{-1}, which is five order of magnitude less than that of NiO. It is interesting to note that the conductivities of the mixtures are also quite different. While NiO rich mixture, i.e. MgO:NiO = 1:2 has a value which is intermediate between those of MgO and NiO, the same does not hold true for MgO:NiO = 2:1. This mixture has almost the same conductivity as pure MgO.

Clearly, in mixtures corresponding to Ni and $MgNi_2$, NiO is the continuous phase with the result that conductivity of the pellet is close to that of NiO. Thus, the pellet in such mixtures benefits from the high conductivity of the host phase. In MgO:NiO = 2:1 mixture, it appears that MgO is the continuous phase and the presence of NiO which occurs as isolated islands, does not exert a pronounced influence on the conductivity. Thus, the conductivity of the MgO rich mixture does not differ significantly from that of pure MgO.

It should be mentioned that with the conductivities measured for MgO and the MgO rich mixture are not unlike those expected for other insulating oxides such as ZrO_2 and SiO_2. The latter oxide, for instance, was reduced quite successfully by Nohira et al. [8] using the contacting electrode method, i.e. increasing the number of contacting points in the cathode. Chen and co-workers [9,10] formalized this by three-phase interline model according to which the reduction proceeds by the propagation of three-phase (conductor/insulator/electrolyte) interlines into the insulator compound. Obviously, this mechanism was not operative in the current samples. The experiments carried out by pellets sandwiched between two contacting metallic plates establishing many contacts with the oxide did not lead to noticeable improvements in the electrolysis.

It is apparent that the oxides in the current system, both MgO and NiO, differ from most of the other oxides in the details of their electro-deoxidation. Electroreduction of oxides such as TiO_2 [26], Nb_2O_5 [27] and B_2O_3 [28], Cr_2O_3 [29] and Ta_2O_5 [30] all involve the formation of intermediate phases which, in the respective order, are $CaTiO_3$, $CaNbO_3$, CaB_2O_4, $CaCr_2O_4$, $CaCr_2O_4$ and calcium tantalates. Thus, the reduction in these oxides is not a direct process but occurs through these intermediaries. This is also true for ZrO_2 and SiO_2 where as mentioned by Peng et al. [31] and Yasuda et al. [32], $CaZrO_3$ and $CaSiO_3$ do form during their electro-deoxidation. The electroreduction of Al_2O_3 to Al [33], as has recently been reported by Yan and Fray [34], similarly, involves the formation of calcium aluminates. Thus, in the three-phase interline where the reduction proceeds, it is not the starting oxide but the intermediate phase, which is in contact with the conductor and the electrolyte. Thus, the formation of intermediate phases such as $CaSiO_3$, $CaZrO_3$ or calcium aluminates is expected to alter the conditions for electroreduction including the local conductivity of the pellet. MgO (and also NiO) in contrast do not form such intermediate phases. Therefore, the insulating nature of MgO is not altered during the electrolysis.

Values of conductivity reported above refer to oxides at room temperature. Since the electrolysis was carried out at elevated temperatures, the applicable values are much higher than those reported above. Conductivities of MgO and MgO:NiO = 2:1 mixtures were measured at temperatures up to 600 °C and are reported in Fig. 9(b). The conductivity of MgO rises to 10^{-9} ohm^{-1} cm^{-1}, and that of MgO:NiO = 2:1 to 10^{-6} ohm^{-1} cm^{-1} at 600 °C. The values measured for MgO are comparable with those reported by Lewis and Wright [35]. The conductivity of NiO on its own was not measured in this study, but the reported values are as high as 10^{-2} ohm^{-1} cm^{-1} at 600 °C [36]. Since NiO can be electrodeoxidized quite successfully at this temperature, the value of 10^{-2} ohm^{-1} cm^{-1} can be taken as a rough measure of the required conductivity. Then to reach this value in MgO, using the temperature dependence of conductivity given by Lewis and Wright [35], the required temperature needs to be as high as 1500 °C.

Electrolysis at elevated temperatures may be employed for Mg compounds of high melting points but for the current compositions of Mg_2Ni and pure Mg, which have the melting points of 760 °C and 650 °C, this approach would not be relevant. Clearly, for successful electroreduction of MgO rich mixtures, it would be desirable to find processing techniques that would render pellets with an acceptable conductivity. Evidently, any processing techniques that would disrupt the continuity of MgO phase would be helpful in this respect. But to increase the conductivity to its highest possible level, it is necessary to develop carefully tailored microstructures in the oxide pellets. One possibility, which might be relevant for MgO:NiO = 2:1, would be to make NiO the host phase, i.e. NiO, though small in its proportions, could be distributed in a manner that could preserve its connectivity while enveloping each and all MgO particles.

4. Conclusions

A study was carried out on the synthesis of Mg–Ni compounds as well as pure Ni and Mg from their oxides using the method of electro-deoxidation. The oxides were in the form of discrete phases NiO and MgO, 3.2 μm and 1.9 μm in size respectively, suitably proportioned to yield Ni, $MgNi_2$, Mg_2Ni and Mg. The oxides were electrolyzed in a eutectic mixture of $CaCl_2$–NaCl solution maintained at a constant temperature (900–600 °C), using a graphite anode at a potential of 3.2 V.

The following can be concluded from the current study:

(i) NiO with positive reduction potential can be reduced quite successfully to a metallic state at temperatures studied in this work. The oxide mixture MgO:NiO = 1:2 can also be electrodeoxidized to a metallic state comprising the phases $MgNi_2$ and Ni.
(ii) MgO rich mixtures are difficult to reduce via electrodeoxidation. The mixture MgO:NiO = 2:1 can be reduced to metallic phases only in small proportions. Difficulties in the reduction of MgO and MgO rich mixtures are attributed to low conductivity of MgO.

Further, the low conductivity of the latter compositions is due to MgO being the continuous phase. It is therefore suggested that the conductivity and thus the reducibility of the oxide mixtures would be improved if NiO could be made the host phase.

Acknowledgements

Support for this work was provided by BAP-03-08-DPT.200305K120920-20 and in part by the FP6 program of the European Commission Project (FP6-200-3-518-271) NESSHY, which we gratefully acknowledge. The authors also thank Volkan Kalem for his help with the conductivity measurements and Cara Murphy Keyman for reading the manuscript.

References

[1] G.Z. Chen, D.J. Fray, T.W. Farthing, Nature 407 (2000) 361.
[2] D. Wang, G. Qiu, X. Jin, X. Hu, G.Z. Chen, Angew. Chem. Int. Ed. 45 (2006) 2384.
[3] R.O. Suzuki, K. Tatemoto, H. Kitagawa, J. Alloys Compd. 385 (2004) 173.
[4] R.O. Suzuki, J. Phys. Chem. Solids 66 (2005) 461.
[5] C.S. Seo, S.M. Jeong, S.B. Park, J.Y. Jung, S.W. Park, S.H. Kim, J. Chem. Eng. Jpn. 39 (2006) 77.
[6] X. Kang, Q. Xu, S.J. Ma, L. Zhao, Q.S. Song, Electrochemistry 77 (2009) 663.
[7] G.Z. Chen, D.J. Fray, T.W. Farthing, Metall. Mater. Trans. B 32 (2001) 1041.
[8] T. Nohira, K. Yasuda, Y. Ito, Nat. Mater. 2 (2003) 397.
[9] X.B. Jin, P. Gao, D.H. Wang, X.H. Hu, G.Z. Chen, Angew. Chem. Int. Ed. 43 (2004) 734.
[10] W. Xiao, X. Jin, Y. Deng, D. Wang, X. Hu, G.Z. Chen, Chem. Phys. Chem. 7 (2006) 1750.
[11] A. Cox, D.J. Fray, Electrochem. Soc. Proceed. 19 (2002) 745.
[12] G. Qui, D. Wang, X. Jin, G.Z. Chen, Electrochim. Acta 51 (2006) 5785.
[13] S. Tan, T. Örs, M.K. Aydinol, T. Öztürk, İ. Karakaya, J. Alloys Compd. 475 (2009) 368.
[14] Z. Yong, M. Meng, W. Dihua, J. Kai, H. Xiaohong, J. Xianbo, G.Z. Chen, Chin. Sci. Bull. 51 (2006) 2535.
[15] A.J.M. Wood, R.C. Copcutt, G.Z. Chen, D.J. Fray, Adv. Eng. Mater. 5 (2003) 650.
[16] X.Y. Yan, D.J. Fray, Adv. Func. Mater. 15 (2005) 1757.
[17] G. Qiu, D. Wang, M. Ma, X. Jin, G.Z. Chen, J. Electroanal. Electrochem. 589 (2006) 139.
[18] L. Zaluski, A. Zaluska, J.O. Stromolsen, J. Alloys Compd. 217 (1995) 245.
[19] L. Lutterotti, S. Matthies, H.R. Wenk, Int. U. Crystallogr. Comm. Powder Diffr. Newslett. 21 (14) (1999), MAUD Version 2.072, 2008 http://www.ing.unitn.it/luttero/maud.
[20] I. Barin, O. Knacke, O. Kubaschewski, Thermochemical Properties of Inorganic Substances, 2nd ed., Springer-Verlag, Berlin, 1973.
[21] C.W. Bale, P. Chartrand, S.A. Degterov, G. Eriksson, K. Hack, R. Ben Mahfoud, J. Melançon, A.D. Pelton, S. Petersen, Calphad 26 (2002) 189.
[22] İ. Karakaya, W.T. Thompson, Can. Met. Q. 25 (1986) 307.
[23] J.J. Peng, G. Li, H. Chen, D. Wang, X. Jin, G.Z. Chen, J. Electrochem. Soc. 157 (2010) F1–F9.
[24] G. Qiu, M. Ma, D. Wang, X. Jin, X. Hu, G.Z. Chen, J. Electrochem. Soc. 152 (2005) E328.
[25] M. Ma, D. Wang, X. Hu, X. Jin, G.Z. Chen, Chem. Eur. J. 12 (2006) 5075.
[26] K. Dring, R. Bhagat, M. Jackson, R. Dashwood, D. Inman, J. Alloys Compd. 419 (2006) 103.
[27] T. Wu, W. Xiao, X. Jin, C. Liu, D. Wang, G.Z. Chen, Phys. Chem. Chem. Phys. 10 (2008) 1809.
[28] T. Örs, S. Tan, T. Öztürk, İ. Karakaya, J. Mater. Sci. 44 (2009) 3514.
[29] D.J.S. Hyslop, A.M. Abdelkader, A. Cox, D.J. Fray, Acta Mater. 58 (2010) 3124.
[30] Q. Songa, Q. Xua, X. Kanga, J. Dub, Z. Xib, J. Alloys Compd. 490 (2010) 241.
[31] J. Peng, K. Jiang, W. Xiao, D. Wang, X. Jin, G.Z. Chen, Chem. Mater. 20 (2008) 7274.
[32] K. Yasuda, T. Nohira, R. Hagiwara, Y.H. Ogata, J. Electrochem. Soc. 154 (2007) E95.
[33] H. Xie, H. Zhang, Y. Zhai, J. Wang, C. Li, J. Mater. Sci. Technol. 25 (2009) 459.
[34] X.Y. Yan, D.J. Fray, J. Appl. Electrochem. 39 (2009) 1349.
[35] T.J. Lewis, A.J. Wright, Br. J. Appl. Phys. D 1 (1968) 441.
[36] S.P. Mitoff, J. Chem. Phys. 35 (1961) 882.